Advanced Composite Materials
Publication details, including instructions for authors and subscription information:
http://www.tandfonline.com/loi/tacm20

Computational analysis of shear thickening fluid impregnated fabrics subjected to ballistic impacts

Bok-Won Lee [a] & Chun-Gon Kim [a]
[a] Department of Aerospace Engineering, KAIST 373-1 Guseong-dong, Yuseong-gu, Daejeon, 305-701, Republic of Korea
Version of record first published: 02 Jul 2012.

To cite this article: Bok-Won Lee & Chun-Gon Kim (2012): Computational analysis of shear thickening fluid impregnated fabrics subjected to ballistic impacts, Advanced Composite Materials, 21:2, 177-192

To link to this article: http://dx.doi.org/10.1080/09243046.2012.690298

Advanced Composite Materials
Vol. 21, No. 2, April 2012, 177–192

Computational analysis of shear thickening fluid impregnated fabrics subjected to ballistic impacts

Bok-Won Lee and Chun-Gon Kim*

Department of Aerospace Engineering, KAIST 373-1 Guseong-dong, Yuseong-gu, Daejeon, 305-701, Republic of Korea

(*Received 4 July 2011; accepted 25 March 2012*)

The impregnation of shear thickening fluid (STF) into high-tenacity fabrics has drawn research attention, because it enhances the ballistic performance of fabrics without inducing loss of flexibility in the fabrics. The performance enhancement provided by the STF is suspected to be due to the increased frictional interaction between yarns in impregnated fabrics. In order to explore the mechanism of this enhanced energy absorption, a computational analysis has been performed to consider the effect of STF impregnation on the ballistic performance of STF impregnated fabrics, and the results are reported here. The computational model to account for STF impregnation was implemented into the explicit analysis code LS-DYNA by employing the experimental results of yarn pull-out tests to characterize the frictional behavior of the STF impregnated fabric. The results of a ballistic impact test were used to validate the computational model that takes into account STF impregnation effect. The computational analysis model proposed here to account for the effect of STF impregnation on the ballistic performance of STF impregnated high-tenacity fabrics is shown to reflect the experimental observations of STF impregnated fabrics subjected to ballistic tests.

Keywords: ballistic impact; shear thickening fluid; computational analysis; frictional characteristics; yarn pull-out

1. Introduction

Woven fabrics made from high-tenacity fibers have been widely used as ballistic protection products. However, they offer a limited level of protection against ballistic threats without reinforcement from heavy and bulky metal or ceramic plates. Recently, research [1–5] into various alternative means of enhancing the ballistic performance of high-tenacity fabrics has been performed. The most common feature of those researches has been the addition of a modifier to the fabric to enhance the efficiency of the interaction of the yarns to defeat the projectile. The impregnation of shear thickening fluid (STF) into high-tenacity fabrics has drawn, attention because it induces little or no increase in the thickness or stiffness of the fabrics [3–5]. However, how the impregnation of STF plays a role in the energy absorption mechanism of the impregnated fabrics is not yet well understood. The essential physics of the impact mechanism associated with STF impregnation into fabrics is difficult to investigate through experimental means alone. In order to complement experimental understanding, a computational analysis of STF impregnated fabrics has been carried out here to investigate the ballistic mechanisms of

*Corresponding author. Email: cgkim@kaist.ac.kr

ISSN 0924-3046 print/ISSN 1568-5519 online

http://dx.doi.org/10.1080/09243046.2012.690298
http://www.tandfonline.com

impregnated fabric armor systems. Although a number of computational studies have been carried out to predict the ballistic performance of fabric armor systems, no other models have been proposed to characterize the STF impregnated fabric armor.

This paper presents a computational model of woven fabric incorporated with the effect of STF impregnation. It has been reported that the primary contribution of STF impregnation in ballistic fabric was the increase of friction between yarns in the fabric that resulted in the enhancement of the energy absorption reflected in experimental observations [3]. Duan et al. [6,7] presented a finite element model that was able to account for yarn sliding and frictional effects between the interwoven yarns of ballistic fabrics. Their parametric study showed that friction between yarns facilitates energy dissipation within the fabric target. Kirkwood et al. [8] proposed a semi-empirical model of the energy absorption in ballistic fabrics by assuming yarn pull-out as the primary energy absorption mechanism. They demonstrated that quasi-static pull-out results can be correlated quantitatively with yarn pull-out during ballistic impact.

In the current study, the nonlinear explicit finite element code LS-DYNA 3D is used to simulate the response of STF impregnated fabric subjected to ballistic impact. Lee et al. [9] conducted ballistic experiments and experimental results were used to investigate the applicability of the proposed model. The frictional behavior of STF impregnated fabric was modeled to be implemented into the computational model by employing the computational and experimental observations of the pull-out behavior of single yarns in STF treated fabric. The results obtained from the computational simulations were verified with those from the experiments [9]. Acceptable agreement between the results of the computational analysis and the ballistic test was obtained in terms of the deformation of the STF impregnated fabric during impact, the residual velocity of the projectile, and the energy dissipated by the fabric. The computational analysis also contributed significantly to a better understanding of the mechanisms involved in the impact and the perforation process of the modeled STF impregnated fabrics.

2. Computational modeling

2.1. Geometrical modeling

STF impregnated woven fabric has a multiscale structure formed of elements ranging from nanoscale particles to macroscale fabric. Figure 1 shows a representation of the multiscale Kevlar KM2® fabric with nanoparticle impregnation. Some research [10] has assumed such fabric to be a macroscopic two-dimensional membrane for the purposes of computer

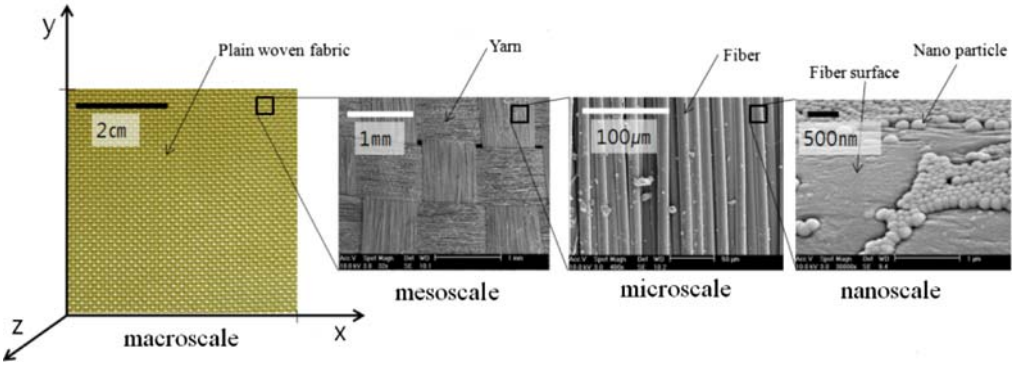

Figure 1. Multiscale representations of KM2® fabric with nanoparticle impregnation.

modeling, although this assumption omits a detailed architecture of the fabric. Recently, models using detailed solid yarn elements have been reported [6,7,11,12]. The full discretization involved in introducing solid yarn elements to computer modeling of the fabrics, however, dramatically increases the computational expense. In order to describe the impregnation effect on the woven fabrics, such models require modeling down to the level of individual yarns. In this study, a mesoscale shell-based finite element model was developed to capture the effect of STF impregnation on the energy absorption mechanism of ballistic fabrics. A yarn was modeled discretely as a continuum and multiple yarns were combined to comprise the fabric. The dimensions of the yarn were extracted from the microscopic image of KM2® yarn shown in Figure 2. The cross section of a yarn interwoven into the fabric was modeled as shown in Figure 3. Table 1 presents values of the geometric dimensions of the cross section and crimp obtained from the microscopic images. Figure 4 shows how the total fabric sample was

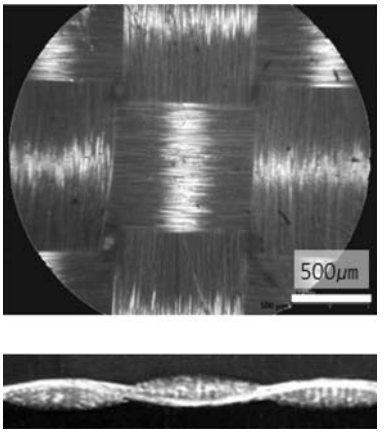

Figure 2. Microscopic image of Kevlar KM2® fabric.

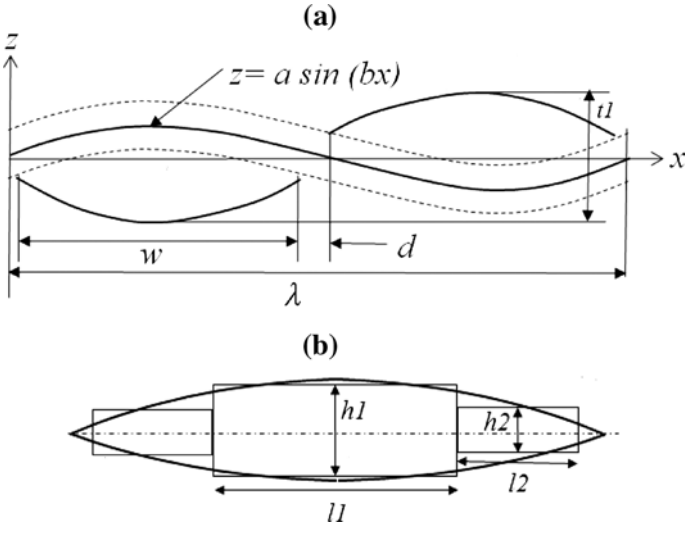

Figure 3. Schematic diagram of a yarn profile of the (a) sinusoidal representation for crimp and (b) the yarn cross section.

Table 1. Geometrical parameters of KM2® yarn.

Parameter	λ	w	d	$t1$	a
Value (mm)	1.64	0.80	0.02	0.22	0.11
Parameter	b	$h1$	$h2$	$l1$	$l2$
Value(mm)	3.83	0.11	0.06	0.38	0.20

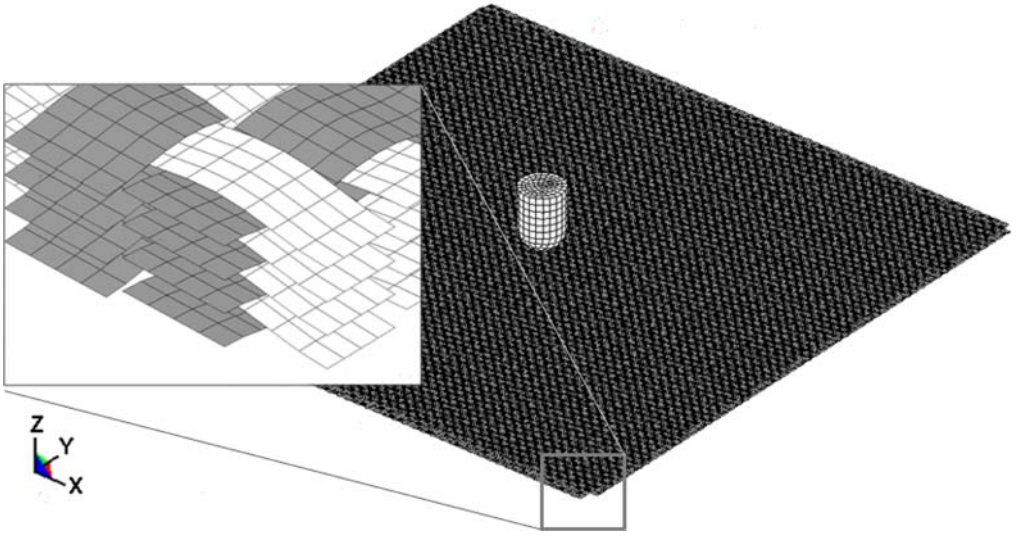

Figure 4. Finite element mesh for the four layers of the KM2® fabric.

modeled by using rectangular cross sections of shell elements to represent the interwoven yarn comprising each of the four fabric layers. The fabric was modeled as having a thickness of 0.22 mm and a yarn crimp wavelength of 1.64 mm. Four shell elements were used to mesh the yarn cross section so as to reasonably represent the cross-section profile. Ten elements were used along a yarn crimp to provide a realistic description of the yarn crimp. A total of 360,000 elements were used to mesh each of the four 100 × 100 mm layers of the fabric. The surface-to-surface contact was introduced between yarns at crossovers, and between the projectile and the fabric. The contact surface of projectile is defined as master surface while slave surface is defined on the fabric. Also, fabric-to-fabric contacts were modeled for multiple layered fabrics so as to be able to simulate the stress waves propagating through multiple fabrics from the impact point. The detailed friction modeling are presented in following chapter.

2.2. Material modeling

The most widely used ballistic fabrics are made of poly-aramid fibers. These fibers typically exhibit viscoelastic behavior and this property becomes significant in high-speed impact problems [10]. Cheng et al. [13] reported the dynamic properties of KM2® fabric using modified Hopkinson bar tests. According to their study, the effects of loading rates on the stress–strain behavior are insignificant over a wider strain rate range for KM2® fiber. The study also

showed that elastic deformation behavior occurred up to failure at 4.5% strain regardless of the loading rate. Thus, LS-DYNA material type 2, orthotropic elastic material, was employed to represent the elastic behavior of KM2® fiber and directional yarn properties considering the volume fraction of the KM2® yarn, as indicated in Table 2. A Von Mises stress of 3.9 GPa was used for the yarn breakage criterion [13].

2.3. Implementation of the effect of the STF impregnation

The computational model developed for the woven fabric was expanded to consider the effect of impregnation with STF. It has been shown through experiments that the major contribution of the STF in the fabric during impact is to increase the friction between the fibers of the fabric. Thus, the frictional behavior in the numerical model must be modified to reflect the frictional behavior of STF impregnated fabrics. Previous experimental and computational studies [1,2,6,7] have shown that modification to the frictional properties of the fabric can greatly alter the yarn pull-out behavior, and often increase the ballistic performance. Therefore, yarn pull-out can be an important energy absorption mechanism during the ballistic impact of fabric. The frictional behavior in LS-DYNA is simply implemented using the Coulomb friction. The frictional coefficient is assumed to be dependent on the relative velocity v_{rel} of the surface in contact as

$$\mu = \mu_d + (\mu_s - \mu_d)e^{-c|v_{rel}|} \quad (1)$$

where μ_d, μ_s, and c are the dynamic coefficient of friction, static coefficient of friction, and exponential decay constant, respectively. In order to correlate the numerical pull-out coefficients with the experimental pull-out data, pull-out simulations were performed using the LS-DYNA model under the conditions shown in Figure 5. The pull-out forces vs. displacement curves obtained from repeated numerical analyses were closely matched with the experimental data by empirically adjusting the parameters in the Coulomb frictional equation, Equation (1). The friction coefficients of the Kevlar KM2® yarn were reported as values of the static coefficient $\mu_s = 0.22$ and the dynamic friction coefficient $\mu_d = 0.20$ [7]. It was necessary to modify these friction coefficients to increase the similarity of the computational analysis to the real phenomena. The LS-DYNA Keyword *User_Interface_Friction subroutines were employed to create more sophisticated frictional models involving the interchange of the relative velocities between the slave node and master node of neighboring yarns. The user subroutine adds the capability of modeling the friction coefficients as a function of the relative sliding velocities according to observations of the experimental pull-out data. The transition of the frictional coefficients after shear thickening activation is accomplished when the sliding velocity between contacted yarn surfaces reaches 1400 mm/min (23.3 mm/s), which corresponds to the onset pull-out speed for shear thickening in experimental observations. Figure 6 shows a comparison of the polynomial fitting curves of the oscillating pull-out force vs. displacement curves obtained from the test and a computational analysis for neat fabric at a pull-out speed of 50 mm/min. It was determined through correlation with the empirical pull-out data that the frictional coefficients for neat Kevlar fabrics in the computational analysis

Table 2. The orthotropic elastic material properties for KM2® yarn.

Parameter	E_{11}	E_{22}	E_{33}	G_{12}	G_{13}	G_{23}	G_{23}	v_{12}	v_{13}	v_{23}
Value (GPa)	63.63	0.98	0.98	0.98	0.98	0.98	0.98	0	0	0

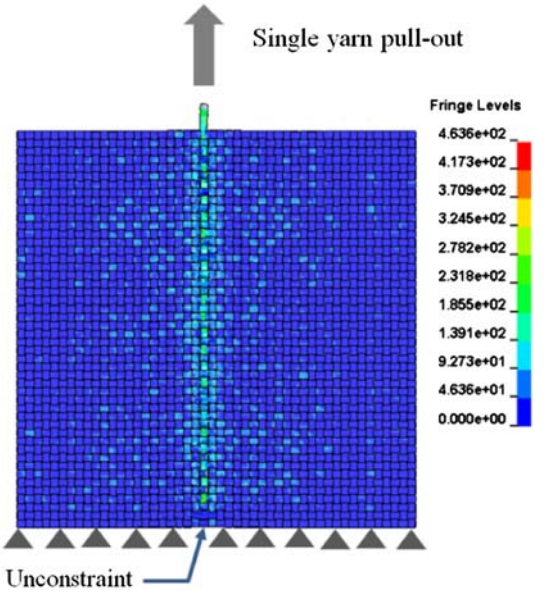

Figure 5. Single yarn pull-out simulation.

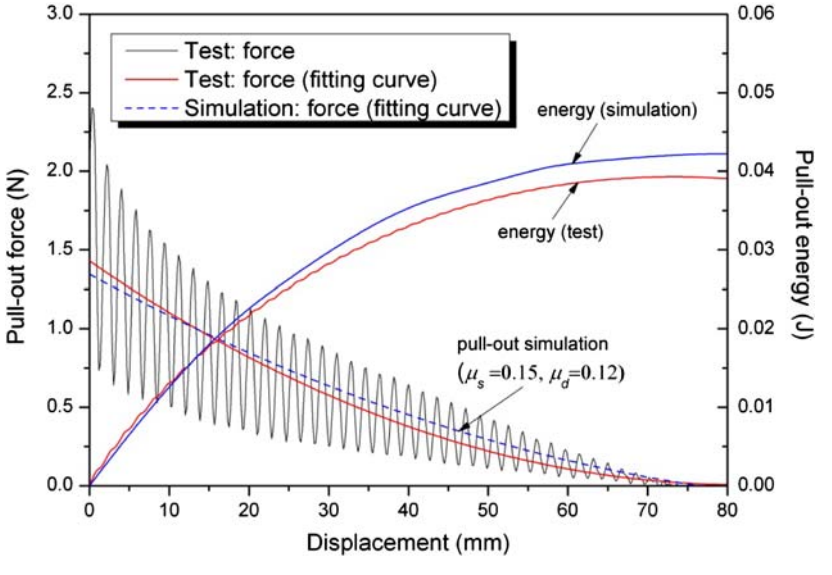

Figure 6. Comparison of the pull-out force and energy of the simulation and experiments for neat fabric at a pull-out speed of 50 mm/min.

should be 0.15 and 0.12 for the static and dynamic coefficients, respectively. By employing similar empirical means, the frictional coefficients at various pull-out speeds were found for both neat and STF impregnated fabrics. Figure 7 shows the semi-empirical frictional model in terms of the relative velocities of the contacted yarn surfaces as a form of Equation (1). There are two distinctive regions showing a significant change of the frictional behavior. The

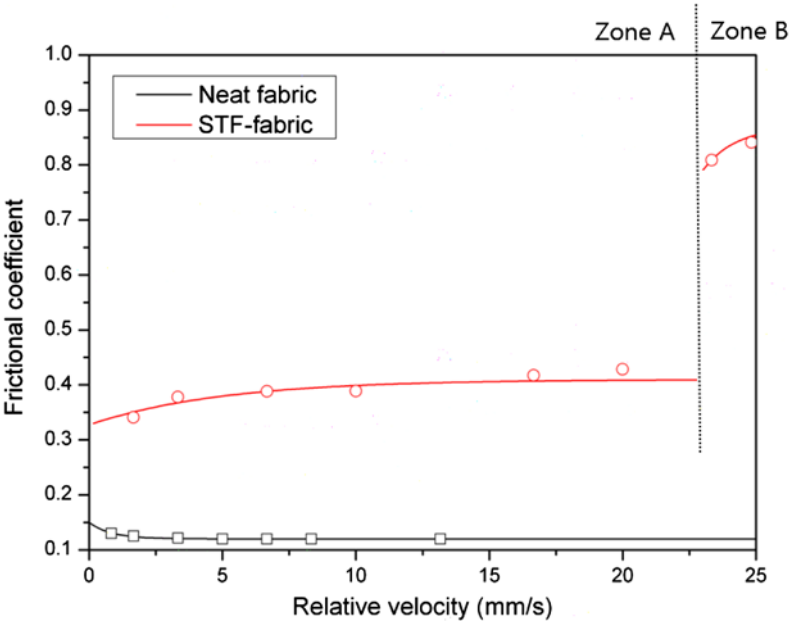

Figure 7. Semi-empirical frictional models for neat and STF impregnated fabrics.

Table 3. Frictional parameters of the semi-empirical friction models.

		STF impregnated fabric	
Parameters	Neat fabric	Zone A	Zone B
μ_s	0.15	0.33	0.79
μ_d	0.12	0.41	0.87
C	1.23	0.21	0.82

pull-out speed range marked as zone 'B' is the range, where shear thickening comes into effect. The obtained coefficients of the Columbo friction model are listed in Table 3.

3. Results and discussion

3.1. Fabric deformations

The enhanced pull-out forces induced by STF impregnation can be modeled by adjusting the frictional parameters in the numerical analysis by employing a friction subroutine that simulates the pull-out behavior of impregnated fabrics that was observed experimentally. This frictional model was employed for the analysis of ballistic impacts. To explore the validity of the computational model in terms of reflecting the effects of the STF impregnation during high speed impact, different views of the fabric deformation sequence are compared in Figure 8. The two-edge clamped fabric models were subjected to 214 m/s ballistic impact with a 7.62 mm spherical bullet. As can be seen in the figure, the global transverse deflection shapes exhibit similar behavior for both neat fabric and STF impregnated fabrics. However, the local fabric structures in the impact region of STF impregnated fabric are well maintained, while

they are significantly distorted for the neat fabric. Notably, significant yarn pull-out is observed at the middle of the free edges connected to the direct impact point for the neat fabric. In contrast, yarn pull-out is hardly observed in the STF impregnated KM2® fabric, as shown in Figure 9. The increased frictional properties induced by STF impregnation restrict the movement of the yarns, thus encouraging neighboring yarns to arrest the projectile. The STF impregnated fabrics are able to maintain their weave integrity during the impact process. Figure 10 shows the transverse deformation profiles of the A-A cross section for neat and STF impregnated fabrics at 80 μs. As can be observed from the figures, transverse structural integrity between layers is significantly increased in STF impregnated fabric when the projectile impinges on a fabric as compared to the neat fabric case. This may be due to the enhanced frictional properties that encourage more yarns to be involved in the arrest of the projectile, while the projectile easily pulls out the contacted yarns and makes an opening by pushing aside the yarn and slipping past the remaining yarns in neat fabric. It was found that the numerical model could reasonably capture the physical impact behavior of KM2® fabrics, while accounting for effect of STF impregnation during high-speed impacts. Figure 11

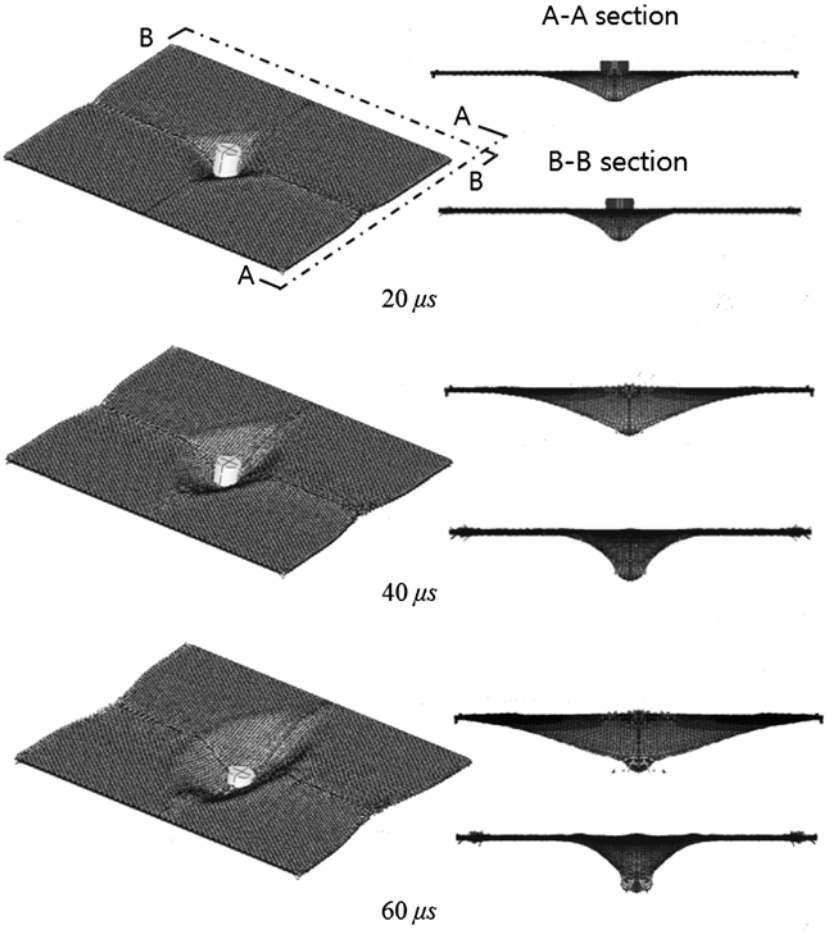

Figure 8. Predicted fabric deformation characteristics of four layers of (a) neat fabric and (b) STF impregnated fabric for impact at 214 m/s.

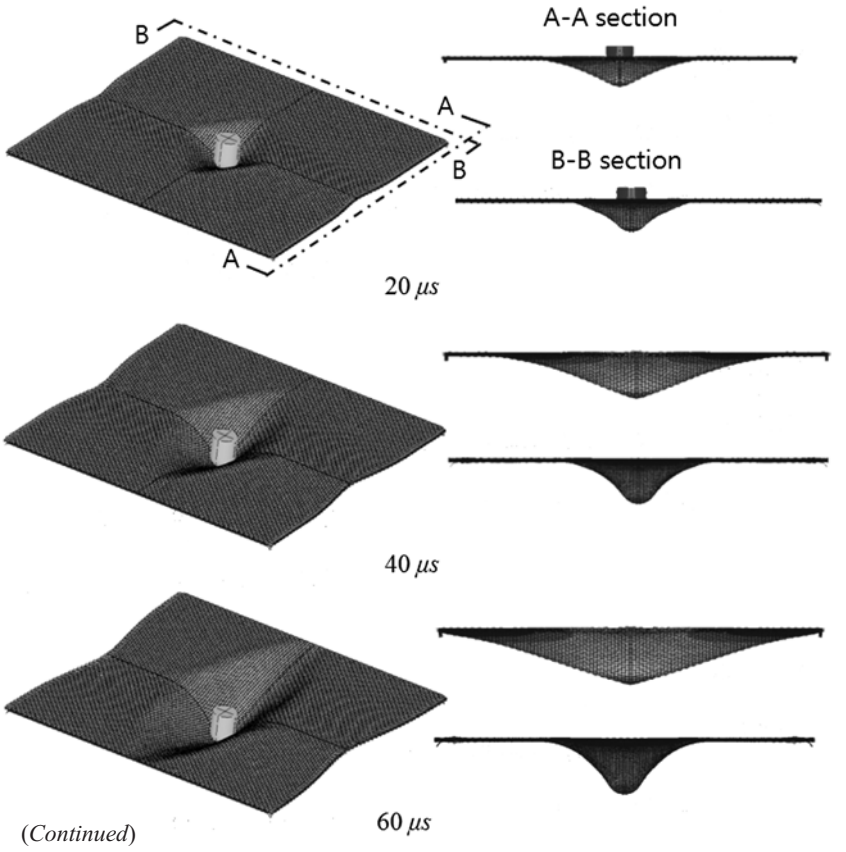

Figure 8. (*Continued*)

presents the variation of projectile velocities with time for four-layered samples of neat and STF impregnated fabrics at an impact velocity of 214 m/s. For neat fabric, the gradient was very gentle due to the yarns pulling out from the weave and slipping off the projectile. The neat fabric offered a lower projectile resistance than the STF impregnated fabric. The rate of decrease in projectile velocities was greater for the STF impregnated fabric than for the neat specimen. The high friction coefficients restrained relative slippage between yarns in the impregnated fabric and encouraged more yarns to be involved in the arrest of the projectile. Figure 12 shows the impact force histories extracted from the element that was directly contacted by the tip of the projectile. The first element failure of the STF impregnated fabric occurred at 80 μs, while it occurred at 50 μs for neat fabric and at 65 μs for the STF impregnated fabric simulated without the benefit of the sudden friction enhancement induced by shear thickening. This implies that frictional properties contribute to retard yarn breakage by helping to maintain the weave structure. This mechanism resulted in the enhancement of the ballistic performance of the STF impregnated fabrics.

3.2. Residual velocities

Figure 13 shows a comparison of the initial and residual velocities of both the experimental and numerical analysis results. The residual velocities were numerically calculated when the velocity difference of the projectile between time step Δt and Δt+1 was less than 1% after penetration. There is good agreement between the numerical and experimental residual

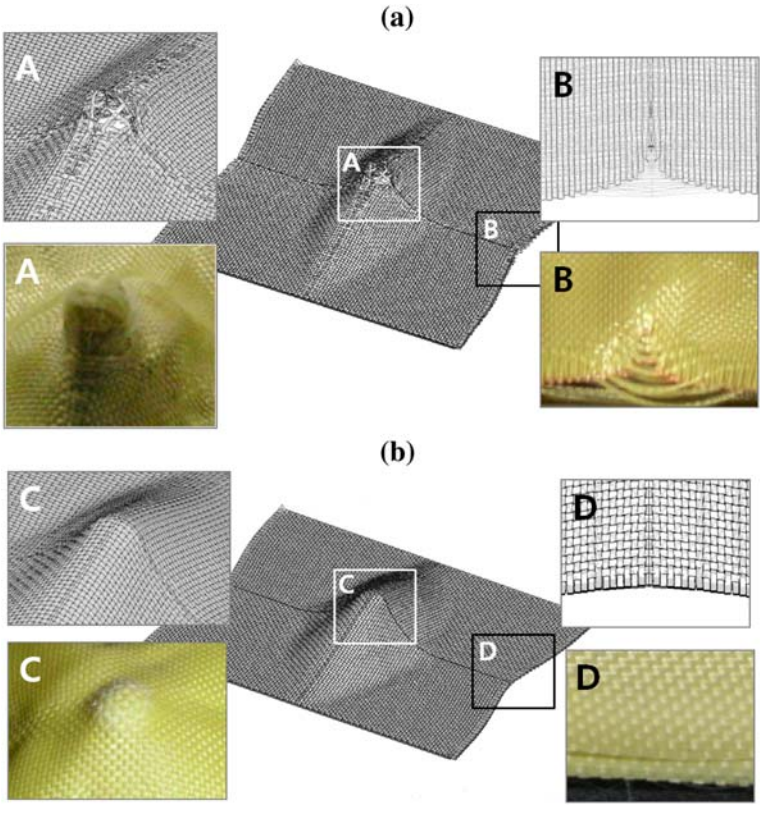

Figure 9. Comparison of the local woven structure and pull-out behavior along the free edges between test specimens and numerical models for (a) neat fabrics and (b) STF impregnated fabrics.

velocities for both neat and STF impregnated fabrics. The experimental and computational analysis results indicate that the effect of the STF tends to diminish at high-impact velocities. For both neat and impregnated fabrics, the residual velocities approach initial velocity as impact velocities are increased. It is noted that experimental ballistic limits of the neat KM2® fabric and STF impregnated fabrics were 71 and 79 m/s, respectively, while the numerical analysis yielded 75 m/s for neat fabric and 86 m/s for STF treated fabric. The energy (E_D) dissipated into the fabrics during ballistic impact can be calculated from the following equation

$$E_D = \frac{1}{2} m_p (v_i^2 - v_r^2) \tag{2}$$

where m_p, v_i, and v_r are projectile mass, initial velocity, and residual velocity, respectively. Figure 14 shows the variation of the energy dissipated by the neat and STF impregnated KM2® fabric as a function of impact velocity. Tan et al. [14] found similar results for the Twaron® fabrics. The energy dissipated by a single layer of neat KM2® fabric in the present experiment is much lower than that dissipated by the single layer of Twaron® in the experiment by Tan et al. due to various parameters employed by their tests, such as the projectile diameter, the areal density of the fabric (Twaron® 280 g/cm^2), and different clamping conditions. However, the overall trends of the variation of energy dissipation according to the impact velocities show good agreement with their conclusion for neat fabric cases. It is noted

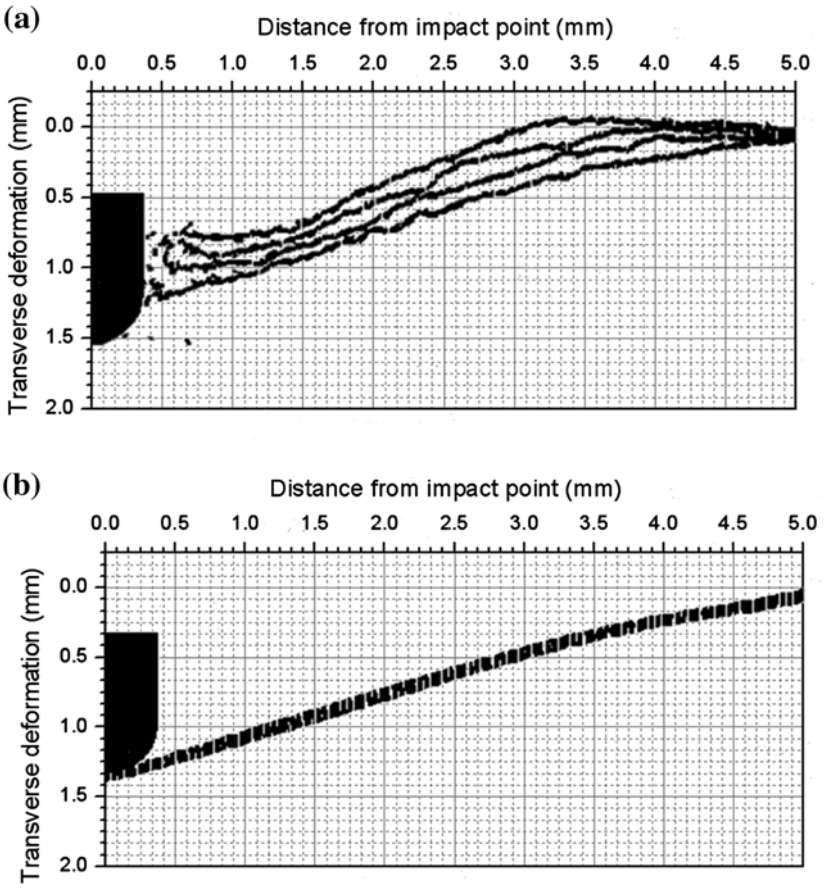

Figure 10. The deformation profiles of the A-A cross section for the (a) neat fabric and (b) STF impregnated fabric.

that the present experimental results show higher energy dissipation than the numerical analysis for both the neat and STF impregnated fabrics. This may be due to the experimental difficulties in achieving perfect clamping or removing wrinkles from the fabric during the clamping. The approach proposed in this present study has some limitations that could affect the accuracy of the results. Microscopy of the impact area after ballistic impact testing showed that the hard colloidal silica particles in the STF make dents and pitting tracks on the softer surface of the fiber, as shown in the nanoscale image in Figure 1. These micromechanical interactions have not been considered in the mesoscale computational model. Another limitation is that the implementation method to account for the effect of the STF impregnation is not able to perfectly capture the frictional behavior between yarns and filaments. The effect of the STF impregnation was implemented based on the results of the pull-out tests. However, pull-out behavior at high strain rates in excess of 1500 mm/min could not be observed due to the crosshead speed limit of the testing machine. Therefore, due to experimental difficulties and limitations, the frictional characteristics implemented in the current model could affect the accuracy of the results. Although the limitations of the computational analysis could yield some discrepancy with the test results, acceptable agreement can be found between the computational analysis and experimental observation.

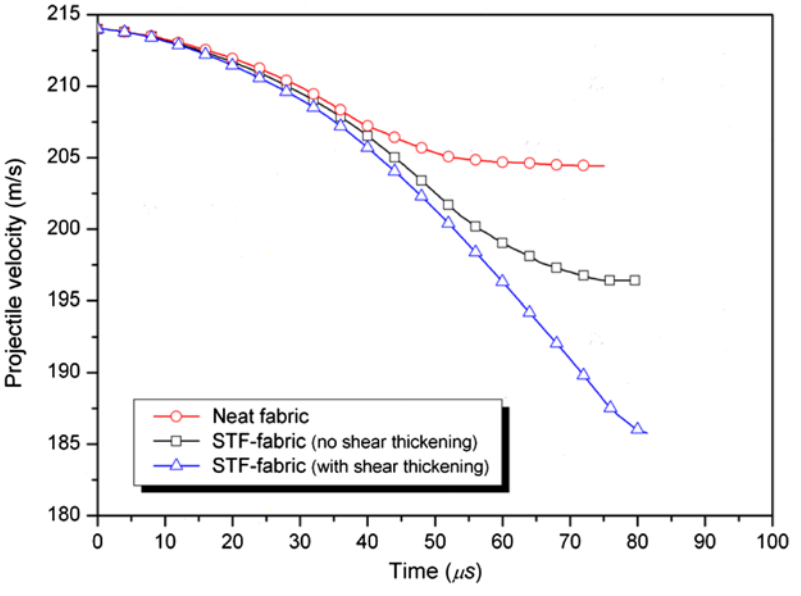

Figure 11. Projectile velocity histories for neat and STF impregnated fabrics.

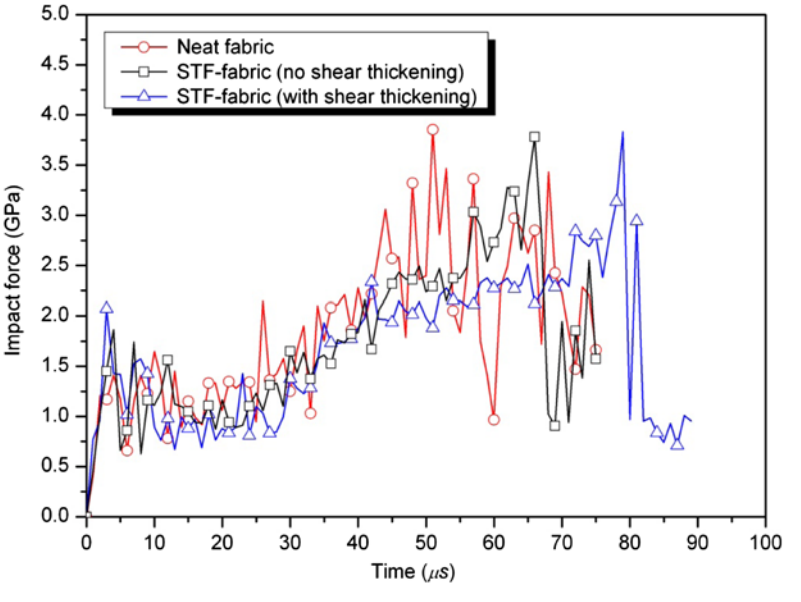

Figure 12. Impact force histories for 214 m/s impact for neat and STF impregnated fabrics.

Both the computational and experimental results showed that the STF impregnation increases energy dissipation as observed in the previous test [9]. STF impregnation offers a particular advantage in the velocity range from 200 to 250 m/s, where the energy dissipation induced by the impregnation exceeds twice that of neat fabric. As velocity increases, the effect of the STF on energy dissipation gradually disappears and almost reaches that of neat

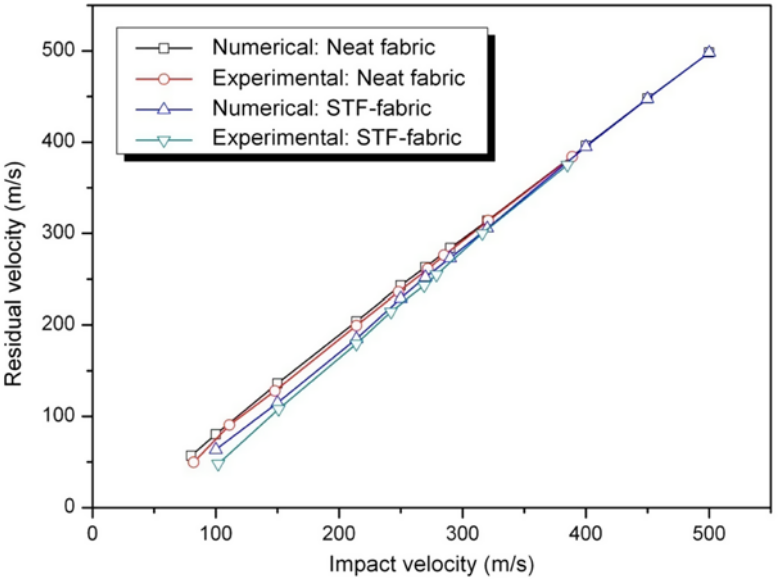

Figure 13. Projectile residual velocities as a function of impact velocity.

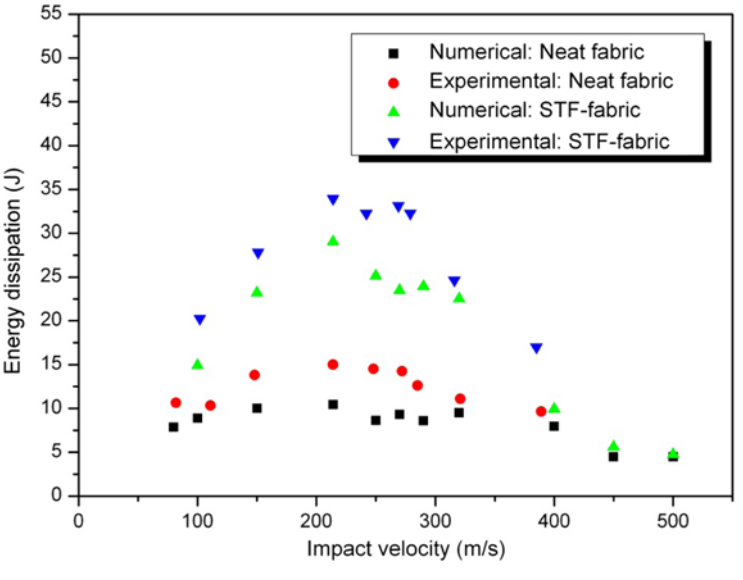

Figure 14. Energy dissipation as a function of impact velocity.

fabric after 400 m/s. This could be explained by observing the penetration shapes of the neat and STF impregnated fabrics for two impact velocities, as shown in Figure 15. The penetration shapes of the numerical analysis of STF impregnated fabric at the impact velocity of 250 m/s reflected many features observed in experimental tests. However, neither the experimental nor the numerical analysis results showed a noteworthy difference in penetration shapes at an impact velocity of 400 m/s, and the transverse deflections of both the neat and

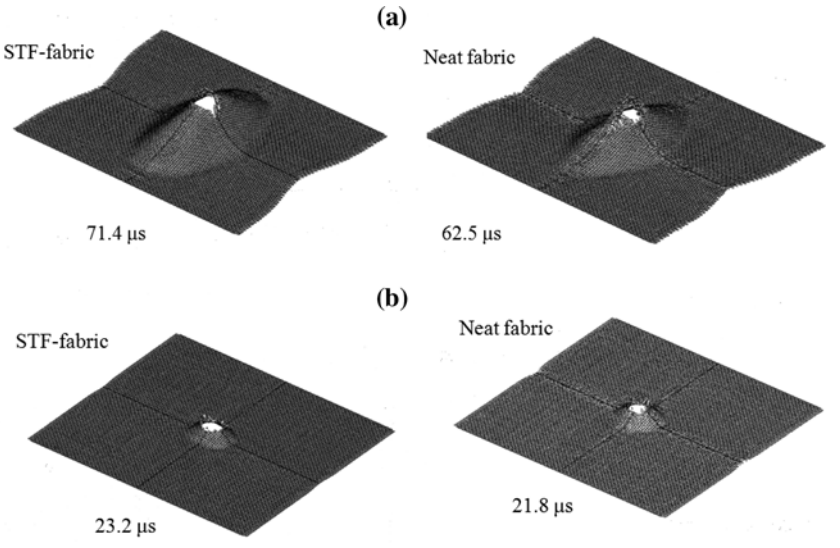

Figure 15. Penetration of the neat and STF impregnated fabrics for impact velocities of (a) 250 m/s and (b) 400 m/s.

impregnated cases were limited to the vicinity of the impact region. At the higher impact velocity, complete penetration was observed before the stress wave could travel across the fabric to transfer the kinetic energy of the projectile. Therefore, the energy absorption mechanism induced by STF impregnation is suspected to be less effective at higher impact velocities. Figure 16 shows the penetration time as a function of the impact velocity. These results correlate well with experimental observation. The results of numerical analysis

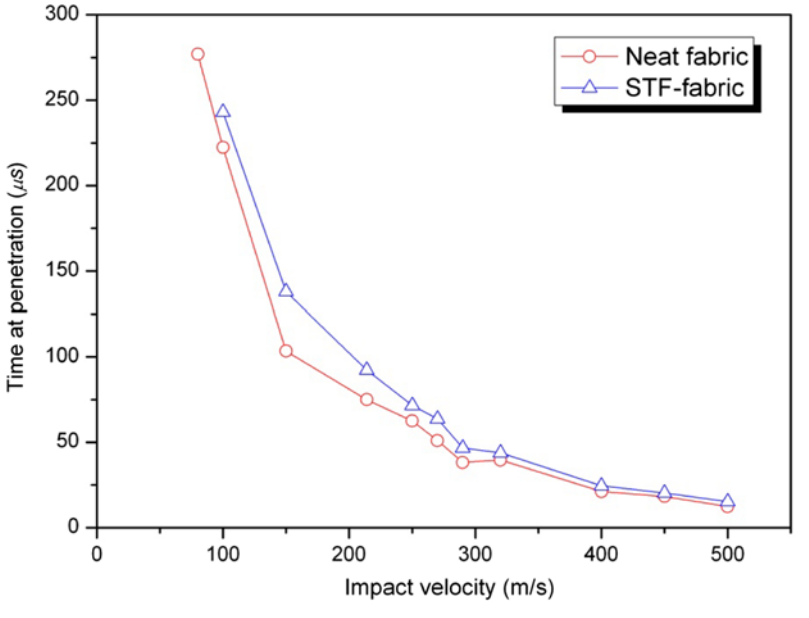

Figure 16. Penetration time as a function of impact velocity.

considering STF impregnation indicated that enhanced friction significantly affects the interaction between the yarns such that local fabric structure is maintained to some extent at the impact region. As a result, STF impregnation allows the projectile to load and break more yarns so that impregnated fabric absorbs more energy than fabric without STF treatment.

4. Conclusions

A computational model of plain woven KM2® fabric impregnated with STF has been shown to predict ballistic responses for the fabric that are in good agreement with ballistic tests. The model is able to reproduce the deformation and damage pattern observed in ballistic tests and to quantitatively agree with the results of the ballistic test in terms of residual velocities. The enhanced energy absorption mechanism induced by impregnation of STF into KM2® fabrics was also investigated. The increased friction induced by STF impregnation encourages a greater interaction between yarns that allows the fabric to maintain its woven structure longer than neat fabric during the impact process. This increased friction is the primary energy absorption mechanism of the enhanced ballistic performance of the STF impregnated KM2® fabric. The proposed computational model to account for the effect of STF impregnation on ballistic fabrics was shown to reasonably represent the physical features of the STF impregnated fabrics when subjected to ballistic impact.

Acknowledgement

This work was supported by the Agency for Defense Development and National Research Foundation of Korea (NRF) grant funded by the Korea government (MEST) (No. 2012-0000133).

References

[1] Gadow R, Niessen KV. Lightweight ballistic with additional stab protection made of thermally sprayed ceramic and cermet coatings on aramide fabrics. International Journal of Applied Ceramic Technology. 2006;3:284–92.
[2] Ahmad MR, Ahmad WY, Salleh WJ, Samsuri A. Performance of natural rubber coated fabrics under ballistic impact. Malysian Polymer Journal. 2007;2:39–51.
[3] Lee YS, Wetzel ED, Wagner NJ. The ballistic impact characteristics of kevlar woven fabrics impregnated with a colloidal shear thickening fluid. Journal of Materials Science. 2004;38:2825–33.
[4] Decker MJ, Halbach CJ, Nam CH, Wagner NJ, Wetzel ED. Stab resistance of shear thickening fluid (STF)-treated fabrics. Composites Science and Technology. 2007;67:565–78.
[5] Tan VBC, Tay TE, Teo WK. Strengthen fabric armour with silica colloidal suspensions. International Journal of Solids and Structures. 2005;42:151–7.
[6] Duan Y, Keefe M, Bogetti TA, Cheeseman BA, Powers B. Modeling friction effects on the ballistic impact behavior of a single-ply high-strength fabric. International Journal of Impact Engineering. 2005;31:996–1012.
[7] Duan Y, Keefe M, Bogetti TA, Cheeseman BA. Modeling the role of friction during ballistic impact of a high-strength plain-weave fabric. Composite Structures. 2005;68:331–7.
[8] Kirkwood JE, Kirkwood KM, Lee YS, Egres RG, Jr, Wagner NJ, Wetzel ED. Yarn pull-out as a mechanism for dissipating ballistic impact energy in Kevlar® KM-2 fabric. Textile Research Journal. 2004;74:939–48.
[9] Lee BW, Kim IJ, Kim CG. The influence of the particle size of silica on the ballistic performance of fabrics impregnated with silica colloidal suspension. Journal of Composite Materials. 2009;43:2679–98.
[10] Lim CT, Shim VPW, Ng YH. Finite-element modeling of the ballistic impact of fabric armor. International Journal of Impact Engineering. 2003;28:13–31.
[11] Talebi H, Wong SV, Hamouda AMS. Finite element evaluation of projectile nose angle effects in ballistic perforation of high strength fabric. Composite Structures. 2009;87:314–20.

[12] Barauskas R, Abraitiene A. Computational analysis of impact of a bullet against the multilayer fabrics in LS-DYNA. International Journal of Impact Engineering. 2007;34:1286–305.
[13] Cheng M, Cheng W. Mechanical properties of Kevlar® KM2 single fiber. Journal of Engineering Materials and Technology. 2005;127:197–204.
[14] Tan VBC, Shim VPW, Zeng X. Modeling crimp in woven fabrics subjected to ballistic impact. International Journal of Impact Engineering. 2005;32:561–74.